the plant journal

SEB Society for Experimental Biology

The Plant Journal (2017) **91,** 950–961 doi: 10.1111/tpj.13618

Tetratricopeptide repeat protein Pyg7 is essential for photosystem I assembly by interacting with PsaC in Arabidopsis

Huixia Yang[1,†], Pin Li[1,2,†], Aihong Zhang[1], Xiaogang Wen[1], Lixin Zhang[1] and Congming Lu[1,2,*]

[1]*Photosynthesis Research Center, Key Laboratory of Photobiology, Institute of Botany, Chinese Academy of Sciences, Beijing 100093, China, and*

[2]*University of Chinese Academy of Sciences, Beijing 100049, China*

Received 13 January 2017; revised 19 May 2017; accepted 1 June 2017; published online 21 June 2017.

*For correspondence (e-mail lucm@ibcas.ac.cn).

†These authors contributed equally to this work.

SUMMARY

Although progress has been made in determining the structure and understanding the function of photosystem I (PSI), the PSI assembly process remains poorly understood. PsaC is an essential subunit of PSI and participates in the transfer of electrons to ferredoxin. However, how PsaC is assembled during accumulation of the PSI complex is unknown. In the present study, we showed that Pyg7 localized to the stromal thylakoid and associated with the PSI complex. We also showed that Pyg7 interacted with PsaC. Furthermore, we found that the PSI assembly process was blocked following formation of the PsaAB heterodimer in the *pyg7* mutant. In addition, the analyses of PSI stability in *Pyg7* RNAi plants showed that Pyg7 is involved in maintaining the assembled PSI complex under excess-light conditions. Moreover, we demonstrated that decreased Pyg7 content resulted in decreased efficiency of PSI assembly in *Pyg7* RNAi plants. These findings suggest that the role of Pyg7 in PSI biogenesis has evolved as an essential assembly factor by interacting with PsaC in *Arabidopsis*, in addition to being a stability factor for PSI as seen in *Synechocystis*.

Keywords: photosystem I assembly, photosynthesis, PsaC subunit, tetratricopeptide repeat protein, Arabidopsis.

INTRODUCTION

Photosystem I (PSI), an essential constituent of the thylakoid membrane and one of the largest and most complex macromolecular assemblies known in nature, catalyzes the final step in photosynthetic electron transport: the oxidation of plastocyanin in the lumen and the reduction of ferredoxin in the stroma of cyanobacteria, algae, and plants (Amunts and Nelson, 2009). More importantly, PSI is an extremely efficient solar energy converter and produces one electron for nearly every photon absorbed (Nelson, 2009). Although progress has been made in determining the structure of PSI and understanding its function, PSI assembly remains poorly understood (Shikanai, 2007; Amunts and Nelson, 2008; Busch and Hippler, 2011; Schöttler *et al.*, 2011; Kargul *et al.*, 2012; Mazor *et al.*, 2015; Qin *et al.*, 2015a; Yang *et al.*, 2015; Suga *et al.*, 2016). In contrast to photosystem II (PSII), the rapidity of PSI assembly and the lack of efficient separation techniques have created difficulty in separating possible intermediates from mature PSI complexes (Ozawa *et al.*, 2010; Schöttler *et al.*, 2011; Schöttler and Tóth, 2014).

Current understanding of PSI assembly derives largely from studies of several putative assembly factors in mutants. The two major subunits of PSI, PsaA and PsaB, bind the primary electron donor P700, the primary acceptor A_0, the secondary acceptor A_1, and the [4Fe-4S] cluster F_x. PSI assembly in *Chlamydomonas reinhardtii* begins with the co-translational integration of PsaB into the thylakoid membrane, followed by the integration of PsaA. The newly formed PsaAB heterodimer then serves as a platform for assembly of the remaining subunits (Wostrikoff *et al.*, 2004; Onishi and Takahashi, 2009). Several factors may be involved in the formation of the PsaAB heterodimer. Hypothetical chloroplast reading frame 3 (Ycf3) is necessary for PSI assembly in cyanobacteria, algae, and plants as a chaperone to assist the assembly of at least PsaA and PsaD on the stromal side (Boudreau *et al.*, 1997; Ruf *et al.*, 1997; Naver *et al.*, 2001; Schwabe *et al.*, 2003). PPD1 may assist

the proper assembly of PsaA and PsaB on the lumen side (Liu *et al.*, 2012; Roose *et al.*, 2014). In addition, Ycf3-interacting protein 1 (Y3IP1) cooperates with Ycf3 during PSI assembly, but only in plants (Albus *et al.*, 2010).

Pyg7, a TPR protein, is orthologous to Ycf37 of *Synechocystis* and CGL71 of *Chlamydomonas* (Wilde *et al.*, 2001; Stöckel *et al.*, 2006; Heinnickel *et al.*, 2016). In *Synechocystis*, deletion of *Ycf37* results in an approximately 30% decrease in PSI content, with no observable change in growth or photosynthetic electron transport and Ycf37 is suggested to stabilize the PSI intermediates under high light conditions (Wilde *et al.*, 2001; Dühring *et al.*, 2006, 2007). In *Chlamydomonas*, CGL71 protects photosystem I from oxidative disruption during assembly (Heinnickel *et al.*, 2016). In *Arabidopsis*, mutation of *Pyg7* leads to the abolition of photoautotrophic growth and an almost complete loss of the PSI complex (Stöckel *et al.*, 2006). Very recently, PSA3 has been shown to promote PSI accumulation in cooperation with Pyg7 (Shen *et al.*, 2017). However, the role of Pyg7 in the PSI complex accumulation remains elusive.

The PsaC subunit of PSI binds two terminal electron acceptors, F_A and F_B, and participates in the transfer of electrons to ferredoxin. PsaC on the stromal side associates with PsaD and PsaE to form the 'stromal ridge' for ferredoxin binding. Moreover, the assembly of PsaC is essential for accumulation of the functional and stable PSI complex (Takahashi *et al.*, 1991; Yu *et al.*, 1995). However, the way in which PsaC is assembled during accumulation of the PSI complex is unknown. To date, no factors specific to PsaC assembly have been reported.

Here, we report that Pyg7 plays an essential role in PSI assembly by interacting with PsaC in *Arabidopsis*. We confirm that Pyg7 is involved in stabilizing the PSI complex under excess-light conditions. These findings suggest that Pyg7 has evolved into an essential assembly factor by interacting with PsaC in plants, as well as conserved as a stability factor as seen in *Synechocystis*.

RESULTS

PSI function and abundance are highly reduced in the *pyg7* mutant

To investigate the role of Pyg7 in the accumulation of the PSI complex, we first thoroughly characterized the function and abundance of PSI in the *Pyg7* knockout mutant *pyg7-2*. The mutant did not survive when grown in soil, but was able to grow heterotrophically on Suc-containing Murashige and Skoog (MS) medium, although seedlings were pale yellowish (Figure S1). The absorbance of P700 at 820 nm was almost undetectable, and electron transport downstream of PSII was blocked (Figures S2a and S2b). The maximum fluorescence emission band peaking at 732 nm in the wild-type (WT) was blue-shifted to 726 nm in the mutant (Figure S2c, Stöckel *et al.*, 2006). The blue shift in *pyg7* could be attributable to the uncoupled LHCI proteins. Moreover, only trace amounts of PSI core subunits (PsaA and PsaC-G) and the PSI complex were detected in the mutant while the levels of Lhca1 and Lhca2 in the mutant still maintained about 1/4 of those in WT (Figure S3), which was similar to previous results (Stöckel *et al.*, 2006). This is probably due to the fact that the PSI antenna proteins accumulate independently of the PSI core subunits (Krech *et al.*, 2012). In addition, the *pyg7* mutant showed a decrease in PSII protein subunits and chlorophyll binding complexes including PSII-RC (D1/D2), core antenna (CP43 and CP47), and peripheral antenna (LHCIIs) (Figure S3). The decrease in PSII protein subunits and chlorophyll binding complexes in *pyg7* may be a secondary effect due to a deficiency in the PSI complex as similar results have been reported in other PSI deficiency mutants (Watkins *et al.*, 2011; Liu *et al.*, 2012). These results indicate that the function and abundance of PSI are highly reduced in the *pyg7* mutant.

The PSI assembly process is blocked in the *pyg7* mutant

Pyg7 is essential for PSI accumulation and acts at the post-translational level by participating in the assembly and/or stability of PSI (Stöckel *et al.*, 2006). Thus, we investigated PSI assembly using *in vivo* [^{35}S]Met pulse-chase experiments followed by blue native (BN)/sodium dodecyl sulfate (SDS)-polyacrylamide gel electrophoresis (PAGE). In these experiments, newly synthesized PsaA and PsaB subunits are [^{35}S]Met-labeled and autoradiographically detected; hence, the assembly steps of PSI can be deduced by monitoring the putative assembly-intermediate complexes containing the newly synthesized PsaA and PsaB proteins. Two-dimensional BN/SDS-PAGE gels stained with Coomassie brilliant blue of isolated thylakoids and PSI core complexes were shown as references to indicate identity of labeled proteins (Figures S4 (left) and S5). To select the appropriate pulse labeling time to allow the chase of assembled complexes, we first [^{35}S]Met-labeled in 5, 10, 20, or 30 min pulses in intact wild-type leaves, then separated the thylakoid proteins using BN/SDS-PAGE (Figure S4 (right)). After a 5-min pulse, no signal for newly synthesized PsaA/B was detected, and only the intensively synthesized D1 protein was detected; mainly as free protein, the PSII reaction center (PSII-RC) complex, and CP43-less monomer. After a 10-min pulse, newly synthesized PsaA/B proteins appeared mainly as free protein (apoprotein and/or monomeric holoprotein) (spot a), while the D1 protein was assembled into larger complexes, such as PSII monomer and dimer. After a 20-min pulse, the newly synthesized PsaA/B was present in several distinct complexes (spots b, c, and d). After a 30-min pulse, some supercomplexes (spot e) were detected. According to the results indicated in Figures S4 (left) and S5, spot d is designed as

the PSI-LHCI supercomplex; spot e represents the supercomplexes that are formed by PSI associated with NDH complexes or/and LHCII complexes (Peng and Shikanai, 2011; Roose *et al.*, 2014; Suorsa *et al.*, 2015); spots b and c stand for the PSI intermediate complexes. The newly synthesized D1 protein existed in several distinct forms including free protein, RC, CP47-RC, CP43-less monomer, PSII monomer, PSII dimer and PSII-LHCII supercomplexes.

Next, using pulse-chase experiments, we compared the PSI assembly process in the WT and *pyg7* mutant. Because the *pyg7* mutant was pale yellowish and grew slowly, we [^{35}S]Met-labeled these with a 30-min pulse to incorporate more radiolabeling in the mutant; we then chased of the PSI assembly process for 0, 15, or 30 min, respectively (Figure 1). In WT, after a 0-min chase, the newly synthesized PsaA/B proteins were assembled into the mature PSI complex (spot d), several intermediate complexes (spots b and c), and the supercomplexes (spot e). However, in *pyg7*, after a 0-min chase, the newly synthesized PsaA/B proteins were assembled into the intermediate complex (spot b) and the trace amount of the mature PSI complex (spot d) while the intermediate complexes (spot c) and the supercomplexes (spot e) were not detected. With increasing chase time, accumulation of the mature PSI complex (spot d) increased in WT while only a faint spot d could be detected in *pyg7*. In addition, the overall labeling of spots a and b in *pyg7* decreased over chase time, indicating an increased turnover of newly synthesized PsaA/B proteins. During the pulse and chase process, the overall pattern of PSII assembly in *pyg7* was similar to that in WT, with the D1, CP43 and CP47 proteins gradually assembled into bigger-sized complexes. These results suggest that the PSI assembly process is blocked in the *pyg7* mutant.

AS several PSI assembly factors, such as Ycf4 and PPD1, accumulate most highly in young leaves (Krech *et al.*, 2012; Liu *et al.*, 2012), we examined the expression pattern of Pyg7 during leaf ontogenesis (Figure S6). Pyg7 content decreased significantly with increasing leaf age, whereas PsaA content remained constant, suggesting that more Pyg7 accumulates in young leaves.

Pyg7 is localized to the stromal thylakoid and associated with the PSI complex

The fluorescence of Pyg7-green fluorescent protein (GFP) specifically matched that of RbcS 1A-GFP, suggesting that Pyg7 was localized exclusively to the chloroplast (Figure S7). To explore the involvement of Pyg7 in the PSI assembly process, we further investigated the sub-

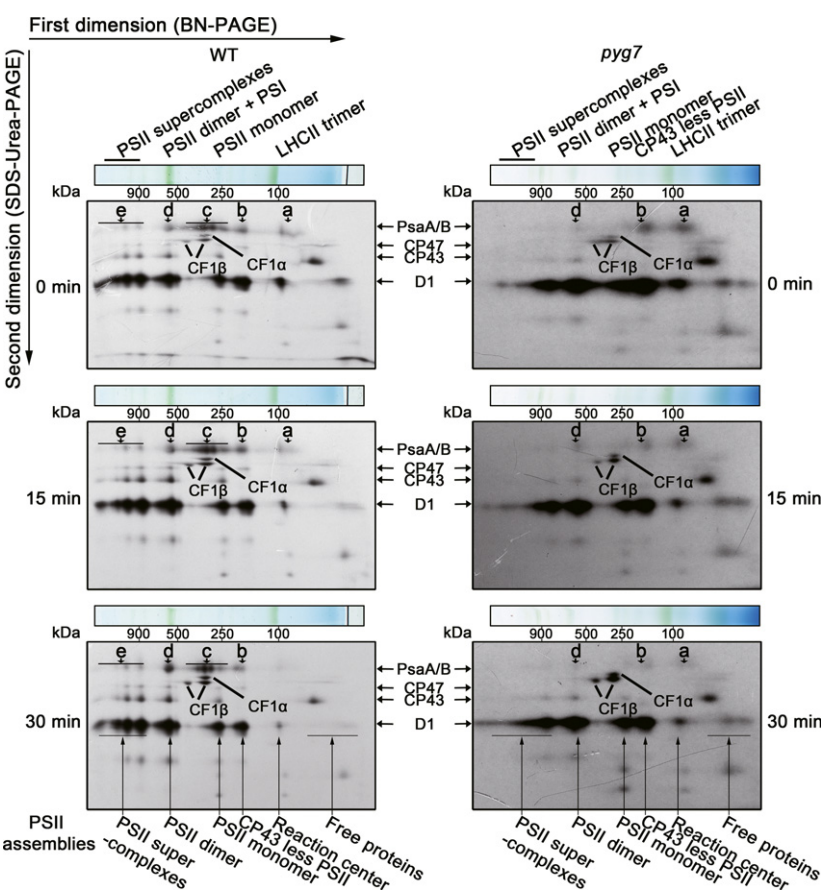

Figure 1. The PSI assembly process is blocked in the *pyg7* mutant.
Leaves detached from 10-day-old seedlings were pre-incubated in the presence of 20 mg ml^{-1} cycloheximide for 30 min, then labeled with 1 μCi μl^{-1} [^{35}S]Met for 30 min. Pulse-labeled leaves were chased for 0, 15, or 30 min, respectively. Thylakoid membrane proteins were separated using blue native (BN) PAGE and subsequent two-dimensional (2D) SDS-PAGE, and visualized by autoradiography. Letters a, d, and e correspond to free PsaA/B proteins, the mature PSI complex, and the supercomplexes, respectively. Letters b and c are designated as the PSI intermediate complexes.

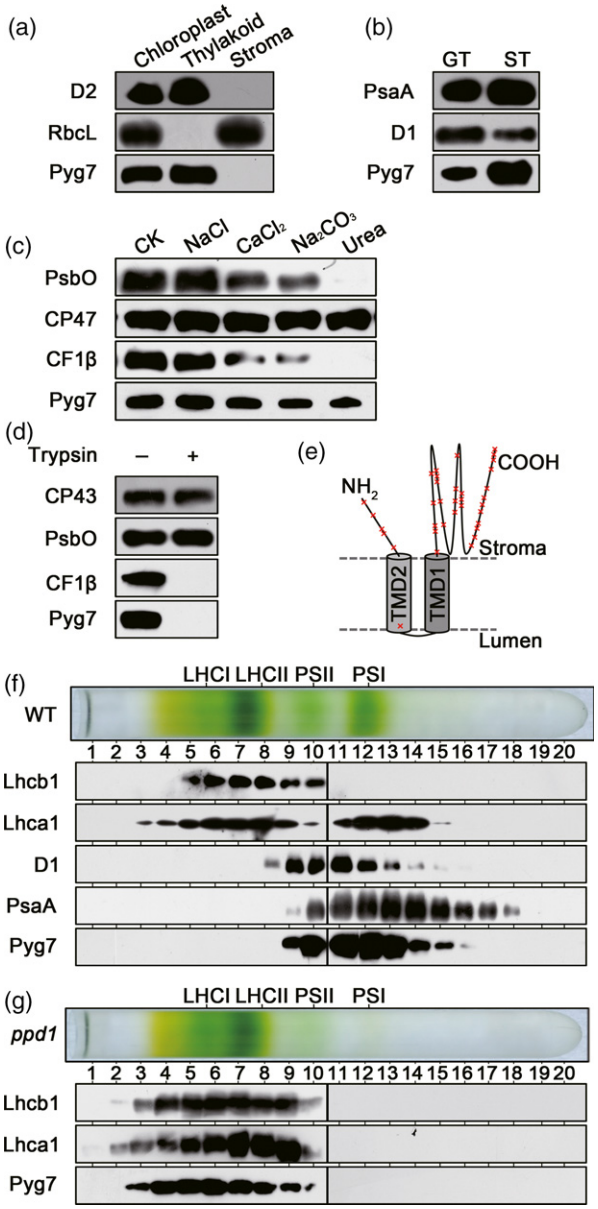

Figure 2. Pyg7 is localized to the stromal thylakoid and associated with the PSI complex.
(a) Pyg7 is a thylakoid membrane protein. Intact chloroplasts were isolated from wild-type (WT) leaves, then separated into thylakoid membrane and stroma fractions.
(b) Pyg7 is mainly localized in the lamellar thylakoid membrane. Intact thylakoid membranes were sub-fractionated into grana thylakoids (GT) and stroma lamellae thylakoids (ST), then subjected to immunoblot analysis.
(c) Pyg7 is tightly associated with the thylakoid membrane. Thylakoids were incubated with various chaotropic agents and used for immunoblot analysis. PsbO, CP47, and CF1β were controls for extrinsic membrane protein in the lumen, integral membrane protein, and peripherally associated protein on the stromal side, respectively. CK, thylakoid membranes not subjected to chaotropic washing.
(d) Pyg7 is a thylakoid protein protruding into the stromal side. Thylakoids were incubated with trypsin. PsbO, CF1β, and CP43 served as controls for thylakoid lumenal proteins, thylakoid stroma proteins, and intrinsic thylakoid membrane proteins, respectively.
(e) Schematic representation of the topology of Pyg7 with two transmembrane regions (TMs), TMD1 and TMD2. Trypsin cleavage sites are indicated by '×'.
(f) Pyg7 co-purifies with the PSI complex. Suc gradient fractions of thylakoids isolated from the wild-type were subjected to immunoblot analysis using the indicated antibodies.
(g) Distribution of Pyg7, the PSI antenna protein Lhca1 and the PSII antenna protein Lhcb1 in the Suc gradient fractions of thylakoids isolated from the *ppd1* mutant with a complete loss of the PSI complex.

localization of Pyg7 within the chloroplast. Chloroplasts from WT leaves were isolated, and separated into soluble and thylakoid membrane fractions. Immunoblot analyses of soluble and thylakoid membrane fractions using marker antibodies revealed that Pyg7 was associated with the thylakoid membrane (Figure 2a), suggesting that Pyg7 is a thylakoid membrane protein. Further sub-fractionation of the thylakoid membrane showed that Pyg7 was mainly localized to the stromal thylakoid membrane (Figure 2b). Analyses of thylakoid membrane incubated with chaotropic salts showed that Pyg7 was associated more tightly with the thylakoid membrane than was CF1β, but not so tightly as CP47, the intrinsic antenna protein of PSII (Figure 2c).

We predicted that Pyg7 would have two transmembrane domains and three tetratricopeptide (TPR) motifs at C-terminal domain (Figure S8; Bohne *et al.*, 2016). To investigate the topology of Pyg7 in the thylakoid membrane, we digested the thylakoid membrane with trypsin, which cannot cross the membrane of intact thylakoids. Immunoblot analyses showed that Pyg7 was sensitive to trypsin digestion, as was the stromal protein CF1β of ATP synthase (Figure 2d). Since the anti-Pyg7 antibody used in this study was raised against a polypeptide at the C-terminal, this result suggests that the C-terminal domain of Pyg7 protrudes out of the stromal side. Considering that there are only 12 amino acids between the two predicted transmembrane domains (Figure S8), it is suggested that the N-terminal domain of Pyg7 also protrudes out of the stromal side (Figure 2e).

We further analysed the localization of Pyg7 using a Suc gradient, in which PSI and PSII were separated after solubilization with dodecyl maltoside (DM). In wild-type plants, Pyg7 was detected in the fractions containing the PSI reaction center protein PsaA and Lhca1 (Figure 2f), which was in agreement with previously reported results (Stöckel *et al.*, 2006). In *ppd1* mutants, with a complete loss of the PSI complex, Pyg7 was detected in the fractions containing Lhca1 (Figure 2g). These results suggest that Pyg7 is associated with the PSI complex.

Pyg7 interacts with PsaC

The above results demonstrate that Pyg7, a stromal thylakoid protein, is essential for PSI assembly and is associated with the PSI complex. Pyg7 contains three TPR motifs

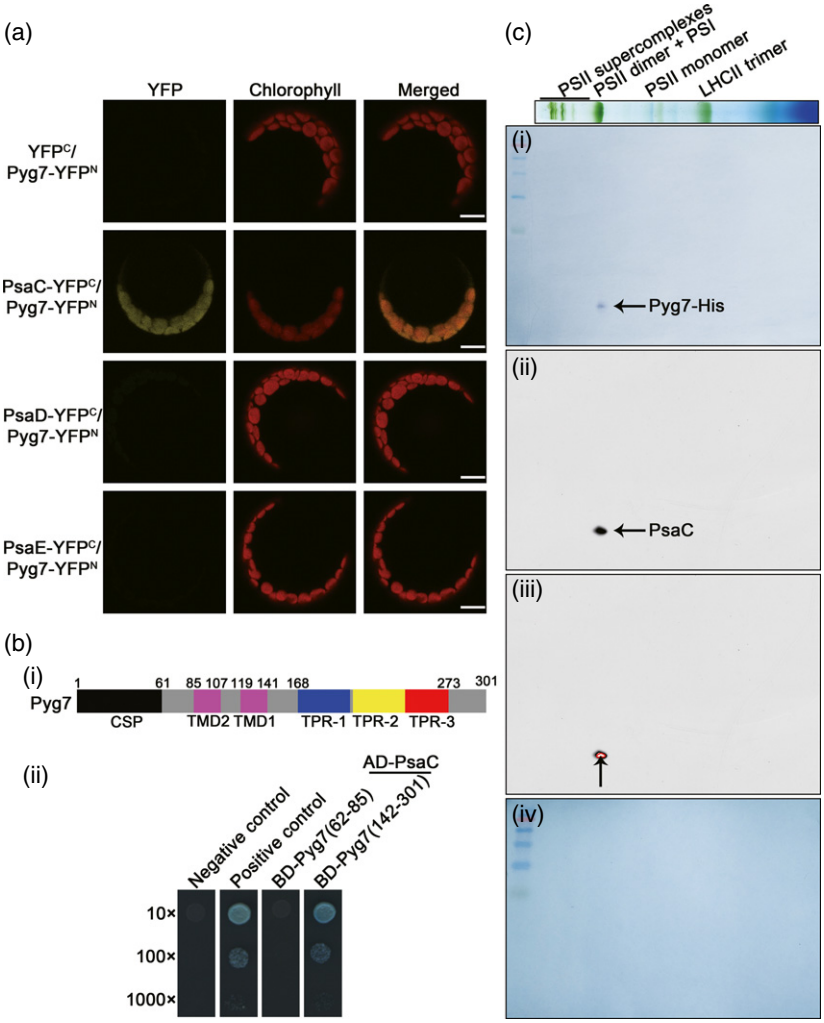

Figure 3. Pyg7 interacts with PsaC.

(a) Interactions between Pyg7 and PsaC *in vivo*, as examined by bimolecular fluorescence complementation (BiFC). No signal was detected from non-fused yellow fluorescent protein $(YFP)^C$ and Pyg7-YFP^N co-expressed in protoplasts as a negative control. Pyg7-YFP^N co-expressed with PsaD-YFP^C and PsaE-YFP^C showed no signal. Co-expression of Pyg7-YFP^N and PsaC-YFP^C showed a YFP signal. Merged panel is the merged view of chloroplast fluorescence and YFP signals. Bars = 5 μm.

(b) Pyg7 tetratricopeptide repeat (TPR)-containing domains are responsible for the interaction with PsaC. (i) Schematic illustration of the topology of Pyg7. CSP, chloroplast signal peptide. TMD, transmembrane domain. TPR, tetratricopeptide repeat domain. Numbers indicate amino acid positions. (ii) Pyg7 TPR domains interact with PsaC, as revealed by yeast two-hybrid assay. The N-terminal region (amino acids 62–85) and the C-terminal region containing TPR domains (amino acids 142–301) were fused as bait constructs. PsaC was fused as the prey construct. AD, Gal4 DNA activation domain; BD, Gal4 DNA-binding domain.

(c) The Pyg7 TPR-containing domain (amino acids 142–301) interacts with PsaC, as revealed by overlay assays. Thylakoid membrane proteins were resolved by 2D BN/SDS-PAGE and transferred to the nitrocellulose membranes. (i) The nitrocellulose membrane was incubated with Pyg7-His fusion protein and subsequently probed with an anti-His tag according to a chromogenic western blot immunodetection kit protocol. (ii) After blotting, the same nitrocellulose membrane was subjected to immunodetection with PsaC antibody as indicated by the arrow by the enhanced chemiluminescence method. (iii) Superposition of (i) and (ii) as indicated by the arrow. (iv) Negative control. After blotting, the nitrocellulose membrane not incubated with Pyg7-His fusion protein was subjected to immunodetection with an anti-His tag using the chromogenic western blot immunodetection kit. Positions of thylakoid complexes are shown at the top of the BN-PAGE gel.

that likely mediate protein–protein interactions (Figure S8; Blatch and Lässle, 1999; Scheufler *et al.*, 2000). Therefore, we expected Pyg7 to interact with some of the PSI subunits on the stromal side. To test this prediction, we investigated the potential of Pyg7 to interact with the three stroma subunits, PsaC, PsaD, and PsaE *in vivo* by bimolecular fluorescence complementation (BiFC), which can directly visualize protein interactions in *Arabidopsis* protoplasts. Yellow fluorescent protein (YFP) signals were observed only in the protoplasts co-transformed by plasmids pUC-SPYNE-Pyg7 and pUC-SPYCE-PsaC, but not in other co-transformed protoplasts; this finding suggests that Pyg7 interacts with the PsaC subunit (Figure 3a). We further determined the Pyg7 domains interacting with PsaC using a yeast two-hybrid

assay. The Pyg7 C-terminal domain, containing three TPR motifs (amino acids 142–301), but not the N-terminal domain (amino acids 62–85), interacted with PsaC (Figure 3b). Overlay assays further confirmed that the Pyg7 C-terminal domain interacts with PsaC (Figure 3c). Taken together, these results suggest that Pyg7 interacts with PsaC with its C-terminal domain.

Pyg7 is involved in maintaining the assembled PSI complex under excess-light conditions

In *Synechocystis*, Ycf37 is suggested to stabilize the PSI intermediate complex under high light conditions (Wilde *et al.*, 2001; Dühring *et al.*, 2006, 2007). Thus, we further examined whether Pyg7 plays a role in protecting the PSI complex from oxidative stress. Since the PSI complex in the *pyg7* mutant was nearly undetectable (Figure S3), we used RNAi to obtain three transgenic lines (*i1*, *i6*, and *i8*) with decreased Pyg7 (Figure S9). Pyg7 content was reduced by about 70, 50, and 30% in *i1*, *i6*, and *i8*, respectively, compared to WT (Figure S9a). Moreover, the decreased Pyg7 content in *i1*, *i6*, and *i8* lines resulted in a corresponding decrease in the levels of PSI subunits (PsaA, PsaC, PsaD, PsaE, and PsaF) and the PSI complex, while PSII subunit (D1, CP43, and Lhcb1) levels were unchanged (Figure S9a, b). There was a corresponding decrease in light-induced P700 absorbance upon illumination at 820 nm (ΔAmax) in the RNAi lines (Figure S9c). To characterize PSI electron transport in the RNAi lines, we investigated the PSI quantum yield, which can be limited either from the donor side or from the acceptor side (Pfündel *et al.*, 2008; Suzuki *et al.*, 2011) (Figure S9d). The effective photochemical quantum yield of PSI, Y(I), was lower in the RNAi lines than in WT. The quantum yield of non-photochemical energy dissipation in PSI caused by limitation on the acceptor side, Y(NA), which is a measure of the level of P700 that cannot be oxidized, was higher in the steady state in RNAi lines than in WT, suggesting that P700 cannot be oxidized efficiently in the RNAi lines. The quantum yield of non-photochemical energy dissipation in PSI caused by limitation on the donor side, Y(ND), which represents the fraction of overall P700 that is oxidized, was very low and largely unchanged in the RNAi lines, indicating that there is no difference in limitation on the donor side between WT and the RNAi lines. Furthermore, the decreased Pyg7 content in *i1*, *i6*, and *i8* lines led to a corresponding decrease in growth (Figure S9e).

We investigated whether Pyg7 is involved in the maintenance of PSI stability under oxidative stress conditions using the RNAi *i1* line. Leaves detached from WT and *i1* plants were exposed to 80 μmol photons m^{-2} sec^{-1} (moderate light, i.e., growth light) and 250 μmol photons m^{-2} sec^{-1} (excess light) for various periods of time up to 30 h in the presence of lincomycin and cycloheximide to inhibit translation in the chloroplast and cytoplasm, respectively. We assessed PSI activity by measuring the maximum photo-oxidizable P700 (ΔAmax). Immunoblotting was used to analyse levels of the PSI subunits PsaA and PsaC (plastid-encoded) and PsaD (nucleus-encoded), and the PetD subunit of the cytochrome b_6f complex (nucleus-encoded). After exposure to moderate light for 30 h, there were no significant changes in ΔAmax, or in the levels of PsaA, PsaC, PsaD, and PetD in either WT or the *i1* line (Figure 4a, c). Under excess light, there was a much greater decrease in ΔAmax with increasing exposure time in the *i1* line relative to WT. After 30 h, there were approximately 20 and 80% decreases in ΔAmax in WT and the *i1* line, respectively (Figure 4b). Levels of PsaA and PsaD were largely unchanged with increasing exposure time in WT, but decreased significantly in the *i1* line. The level of PetD remained unchanged in both WT and the *i1* line (Figure 4d). These results suggest that Pyg7 is required for the stability of the assembled PSI complex under excess-light conditions.

We also determined PSII activity (F_v/F_m) and the content of the PSII core protein D2 in the presence of lincomycin and cycloheximide in WT and the *i1* line under moderate and excess-light conditions (Figure S10). F_v/F_m and the D2 level decreased significantly in WT and the *i1* plant after exposure to moderate and excess light for 30 h. However, there were no significant differences in the decreased extents of F_v/F_m and the D2 level between WT and the *i1* line either under moderate light conditions or under excess-light conditions.

We further investigated the PSI assembly process using *in vivo* pulse-chase experiments in the RNAi lines as described above (Figure S11). After a 20-min pulse, newly synthesized PsaA/B proteins were assembled into several intermediate complexes (spots b and c), the mature PSI complex (d), and the supercomplexes (spot e) in WT and the *i1* line. After a 15-min chase, almost all of the free PsaA/B proteins (spot a) were assembled into the mature PSI complex (d) and possible intermediate complexes (spots b and c) in WT, whereas some PsaA/B free proteins remained in the *i1* line. These results demonstrate that decreased Pyg7 content results in decreased efficiency of PSI assembly, further supporting the conclusion that Pyg7 is required for the PSI assembly process.

DISCUSSION

PSI assembly is a highly ordered process monitored by networks of auxiliary proteins, but the individual assembly steps and the role of transiently acting assembly factors are poorly understood. The use of PSI deficient mutants will provide insights into the mechanism of the PSI assembly. In this study, we found that the absence of Pyg7 resulted in an almost complete loss of PSI core subunits (PsaA–G) and of the PSI complex in Arabidopsis (Figure S3; Stöckel *et al.*, 2006). In order to understand how Pyg7 is

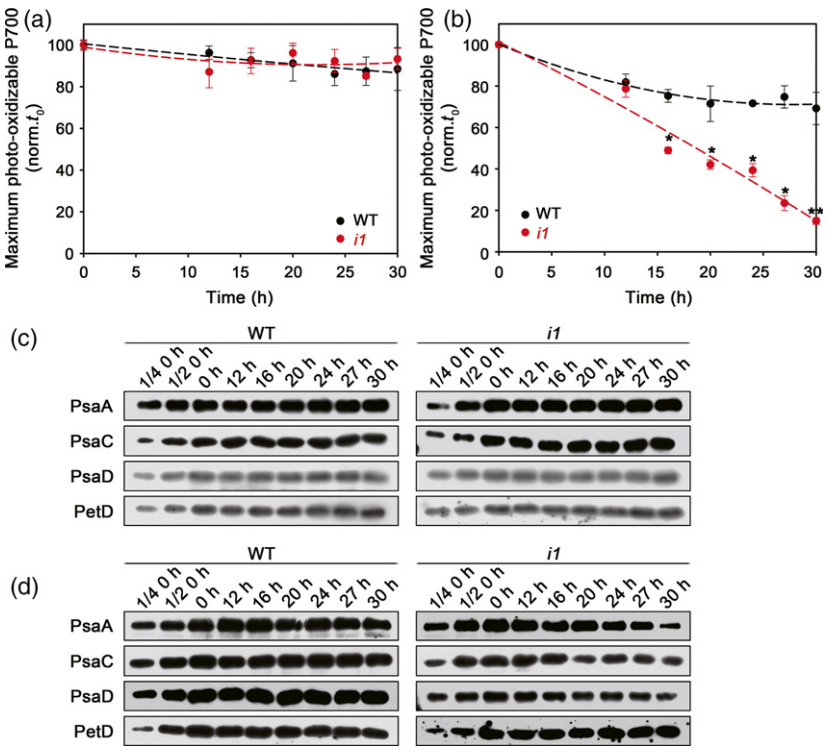

Figure 4. PSI stability analysis in the wild-type and *Pyg7* RNAi *i1* line.
(a, b) Maximum level of photo-oxidizable P700 (ΔAmax; normalized to initial values at time zero, t_0). Leaves detached from wild-type (WT) and the *i1* line in the presence of lincomycin and cyclohexamide were exposed to moderate light (80 μmol photons m^{-2} sec^{-1}) (a) and excess light (250 μmol photons m^{-2} sec^{-1}) (b) for up to 30 h. Data represent means ± standard deviation (SD) (n = 3). Significant difference from the wild-type was calculated using Student's *t*-test (*, $P < 0.05$; **, $P < 0.01$).
(c, d) Immunodetection of specific thylakoid membrane proteins. Leaves detached from WT and the *i1* line in the presence of lincomycin and cyclohexamide were exposed to moderate light (80 μmol photons m^{-2} sec^{-1}) (c) and excess light (250 μmol photons m^{-2} sec^{-1}) (d) for up to 30 h.

involved in PSI assembly, we investigated whether Pyg7 interacts with some subunits of the PSI complex. Our results showed that Pyg7 interacts with PsaC but not with PsaD and PsaE (Figure 3a). The C-terminal domain of Pyg7 has three TPR motifs (Figure S8). We thus further examined if the C-terminal domain of Pyg7 interacts with PsaC. Indeed, we found that the Pyg7 C-terminal domain interacted with PsaC (Figure 3b, c). As the classical function of TPR proteins is to hold different proteins together (Das *et al.*, 1998; Blatch and Lässle, 1999; Scheufler *et al.*, 2000), an interaction of Pyg7 with PsaC indicates that Pyg7 is involved in PSI assembly.

We further investigated how Pyg7 is involved in PSI assembly using *in vivo* [^{35}S]Met pulse-chase experiments. Our results revealed that the newly synthesized PsaA/B protein was assembled into an early intermediate complex (spot b) which could be efficiently assembled further into the PSI-LHCI supercomplex (spot d) and the bigger-sized PSI intermediate complexes (spots c and e) in WT but not in the *pyg7* mutant (Figure 1). Since the molecular mass of this early intermediate complex (spot b) was approximately 160 kDa and we observed that Pyg7 interacts with PsaC (Figure 3), it is suggested that spot b should stand for the PsaAB heterodimer. Therefore, our results suggest that the PSI assembly process is mostly blocked following formation of the PsaAB heterodimer in the *pyg7* mutant. Although the PsaAB heterodimer could be formed in the *pyg7* mutant, other subunits could not be assembled into the mature PSI complex possibly due to the blocking of the PsaC assembly. In *Chlamydomonas*, it is proposed that PsaB is synthesized first acting as an acceptor for the assembly of other PSI subunits, and PsaA integrates with PsaB to form the PsaAB heterodimer and then PsaC is subsequently assembled on the stromal side of the PsaAB heterodimer (Wollman *et al.*, 1999; Wostrikoff *et al.*, 2004). Deletion of PsaC allows the formation of the PsaAB heterodimer in *Synechocystis* sp. PCC6803 (Yu *et al.*, 1995), suggesting that the assembly of PsaC is critical to the accumulation of the stable PSI complex. Thus, the results in this study suggest that Pyg7 is essential for PSI assembly by interacting with PsaC during the assembly process of the PSI-LHCI supercomplex.

In this study, we could not provide direct evidence to support the involvement of Pyg7 in PsaC assembly because it is still unclear which PSI assembly intermediates contain PsaC and whether or not PsaC is present in spot b as shown in Figure 1. The difficult to detect the PsaC signal by autoradiograph may be due to the resolution of SDS-PAGE system used in this study. To confirm the role of Pyg7 in PsaC assembly, it is necessary to investigate the presence of or absence of PsaC in spot b as well as spots d and e in WT and *pyg7*. Thus, the SDS-PAGE system adapted for separation of small proteins or immunoblotting using anti-PsaC antibody instead of autoradiograph could be employed to detect which PSI assembly intermediates contain PsaC.

As discussed above, Pyg7 is involved in PSI assembly by interacting with PsaC during the assembly process of

the PSI complex. Thus, Pyg7 should interact transiently with PsaC and not be associated with the PSI complex. However, the results in this study as well as in a previous study showed that Pyg7 remained associated with the PSI complex (Figure 2f; Stöckel *et al.*, 2006). It seems that Pyg7 is not associated with the LHCI antenna as Pyg7 is involved in the early step of PSI assembly, although Pyg7 was detected in the fractions containing the PSI antenna protein Lhca1 (Figure 2f, g). It has been reported previously that Ycf3 and Ycf4, two PSI assembly factors, are not associated with the PSI complex (Boudreau *et al.*, 1997) and PPD1, a PSI assembly factor by interacting with PsaA and PsaB, is partially associated with the PSI complex (Liu *et al.*, 2012). In addition, PAM68, a PSII assembly factor that interacts with several of the PSII core subunits, is not associated with the PSII complex (Armbruster *et al.*, 2010). Alb3.2, an assembly factor for photosystems, interacts with the reaction center polypeptides of PSII and is associated with the PSII complex (Göhre *et al.*, 2006). It is unclear how Pyg7 functioned as an assembly factor but remained associated with the mature PSI complex. However, our results showed that Pyg7 is required for the stability of the assembled PSI complex under excess-light conditions (Figure 4). Since PsaC contains two terminal electron acceptors, F_A and F_B, which are sensitive to excess light stress (Tiwari *et al.*, 2016), one possible explanation for Pyg7 remained to be associated with the PSI complex is that Pyg7 may be involved in maintaining the assembled PSI complex by protecting PsaC under excess-light conditions.

Our results showed that a decrease in Pyg7 content led to a proportional decrease in the function and abundance of PSI in *Pyg7* RNAi lines (Figure S9). It would be expected that the lower the assembly of PSI, the lower the acceptor side limitation of PSI, since the ratio of PSI to its pool of electron acceptors would decrease, thereby alleviating limitation in electron transfer out of PSI. However, we observed that there was a higher acceptor side limitation of PSI in these RNAi lines than in wild-type plants (Figure S9d). Similar results were observed in the mutants with deficient phylloquinone, the secondary electron acceptor of PSI (Wang *et al.*, 2017). Therefore, something must be happening on the acceptor side of PSI in these RNAi lines. It was previously reported that the F_A/F_B Fe-S clusters are highly sensitive to O_2 when exposed to the atmosphere by the removal of the C terminus of PsaC (Jagannathan and Golbeck, 2009). There is a requirement for shielding the F_A/F_B Fe-S clusters from O_2 exposure by stabilizing PsaC. Since Pyg7 remains associated with the mature PSI complex (Figure 2f; Stöckel *et al.*, 2006), it seems that Pyg7 is not simply a PSI assembly factor, but it is also important for protecting the assembled PSI complex from O_2 disruption by stabilizing PsaC. Thus, the Pyg7 level in the RNAi lines may be not efficient to protect the F_A/F_B Fe-S clusters from O_2 exposure, thereby resulting in an inhibition of electron transfer at the acceptor side of PSI in the RNAi lines.

It should be noted that a faint spot d was observed in the *pyg7* mutant after pulse-labeled leaves were chased for 0, 15, and 30 min (Figure 1), suggesting that trace amount of the mature PSI complex could be assembled. In fact, trace amounts of PSI subunits and the PSI complex were detected in the *pyg7* mutant (Figure S3). These results indicate that other factors involved in PSI assembly may exist during PSI assembly.

Our results showed that Pyg7 content decreased significantly with increasing leaf age, whereas the accumulation of PSI remained largely unchanged (Figure S4), suggesting that Pyg7 accumulated most highly in young leaves. Understandably, the assembly of the PSI complex in young leaves is more required than in mature leaves. Thus, the Pyg7 abundance is higher in young leaves than in mature leaves. It remains unclear why PSI is stable in mature leaves that accumulate much less Pyg7 (Figures 4 and S6). Normally, the PSI assembly process takes place actively in young leaves where more PSI assembly factors are required. The less Pyg7 accumulation in mature leaves (Figure S6) suggests that Pyg7 is required for PSI assembly but not for PSI stability under normal light conditions. Our results indeed show that Pyg7 is involved in PSI assembly (Figure 1). However, Pyg7 is required to stabilize PSI complex under strong light conditions (Figure 4). Therefore, PSI is stable in mature leaves though they accumulate much less Pyg7 under normal light conditions (Figures 4 and S6).

Pyg7 in *Arabidopsis* and CGL71 in *Chlamydomonas* are of common phylogenetic origin; their homolog in *Synechocystis* is Ycf37 (Figure S8). Although these three proteins are all involved in PSI complex accumulation, it seems that their functions differed during evolution. In *Synechocystis*, Ycf37 is suggested to stabilize the PSI intermediates under high light conditions (Wilde *et al.*, 2001; Dühring *et al.*, 2006, 2007). In *Chlamydomonas*, CGL71 also acts as a stabilizing factor to protect the assembled PSI complex against oxidative damage (Heinnickel *et al.*, 2016). In addition, *cgl71* mutants show nearly no accumulation of the PSI complex under dark, oxic conditions, suggesting that CGL71 is essential for PSI assembly although it remains unknown how CGL71 is involved in PSI assembly (Heinnickel *et al.*, 2016). In this study, our results showed that Pyg7 is required to stabilize the PSI complex under excess-light conditions (Figure 4). More importantly, we demonstrated that Pyg7 is an assembly factor that is essential for PSI assembly in *Arabidopsis*. This indicates that similar to CGL71 in *Chlamydomonas*, Pyg7 has evolved from being a stabilizing factor for PSI complex in *Synechocystis* into a crucial assembly factor for the PSI complex in *Arabidopsis*, probably because other, more specific assembly factors were required to assist PSI core subunit assembly during evolution.

EXPERIMENTAL PROCEDURES

Plant materials and growth conditions

The *Arabidopsis thaliana* (ecotype Columbia-0) T-DNA insertion line *pyg7-2* (CS807379) was obtained from the Arabidopsis Biological Resource Center (ABRC; http://abrc.osu.edu/). The T-DNA insertion site was confirmed using the polymerase chain reaction (PCR; for primers used, see Table S1). Homozygous mutant lines were obtained via segregation of the heterozygous plants. WT and heterozygous seeds were sown on MS medium containing 2% sucrose and 0.4% phytagel. After vernalization at 4°C for 2 days, seeds were transferred to a culture chamber under a light intensity of 5 μmol m^{-2} sec^{-1} at 22°C, with a 10-h light/14-h dark period.

Creation of *Pyg7* RNAi lines

For the *Pyg7* RNAi vector construct, a fragment of *Pyg7* (346 bp in size) was subcloned into the cloning sites of pHANNIBAL (Wesley *et al.*, 2001) using forward and reverse primers (see Table S1) to create an inverted repeat transgene separated by the pdk intron. After building the construct and verifying it by sequencing, the transformation cassette was spliced out of the pHANNIBAL vector with *Not*I, then ligated into the *Not*I site of the binary plasmid pART27 (Gleave, 1992). The resulting construct was mobilized into *Agrobacterium tumefaciens* strain GV3101, as described previously (Liu *et al.*, 2012). The floral-dip method was used to produce transgenic plants (Clough and Bent, 1998). Individual transgenic plants were selected on the basis of resistance to 50 mg/L kanamycin on MS medium agar plates. Transgenic kanamycin-resistant seedlings were transferred to soil and grown in a growth chamber at 22°C under a light density of 80 μmol m^{-2} $sec^{-1}$with a 10-h light/14-h dark period. Three transgenic lines, named *i1*, *i6* and *i8*, were selected for further experiments.

Measurement of chlorophyll fluorescence and 77K fluorescence emission spectra

Chlorophyll fluorescence and 77K fluorescence emission spectra were determined using the method described previously (Liu *et al.*, 2012).

P700 redox kinetics

As described by Meurer *et al.* (1996), a PAM 101 fluorometer (Heinz-Walz, Effeltrich, Germany) equipped with an emitter-detector unit (ED 800T) was used to assess P700 redox kinetics by monitoring its absorbance at 820 nm. P700 absorbance changes at 820 nm, induced by far-red (FR) light, represent the relative amounts of photo-oxidizable P700. Intact leaves were dark-adapted for 20 min prior to measurement. P700 oxidation took place on illumination with FR light (720 nm, 24 μmol m^{-2} sec^{-1}). Maximum photo-oxidizable P700 content (ΔAmax) was induced using a 800 msec saturating pulse (625 nm, 2300 μmol m^{-2} sec^{-1}) in continuous FR light.

Determination of PSI complementary quantum yields

The measurements of PSI complementary quantum yields were performed using Dual-PAM-100 (Heinz-Walz, Effeltrich, Germany) (Pfündel *et al.*, 2008). Three types of PSI complementary quantum yields of energy conversion were measured simultaneously with a P700 induction curve. The P700 signal represents the difference of the 875 nm and 830 nm transmittance signals. The leaves of the 3-week-old WT and *pyg7* mutant were dark-adapted for 20 min prior to measurement. The maximal change of P700 signal (P_m) was measured through application of a 200 ms saturation pulse (625 nm, 10 000 μmol m^{-2} sec^{-1}) after a 10 sec FR light (720 nm, 20 μmol m^{-2} sec^{-1}) preillumination. P_o was determined at the end of the 1 sec dark interval following saturation pulse. At 40 sec after FR-off, then actinic light (AL, 625 nm, 80 μmol m^{-2} sec^{-1}) was turned on. In the presence of actinic light, P_m' was induced by a 200 msec saturating pulse (625 nm, 10 000 μmol m^{-2} sec^{-1}) applied every 20 sec. The P700 signal (P) was recorded just before a saturation pulse. The P700 induction curve was recorded for 350 sec to achieve a steady state of the photosynthetic apparatus, and the actinic light was then turned off. Parameters were calculated automatically (Klughammer and Schreiber, 2008):

$$Y(I) = (P'_m - P)/P_m, Y(\mathrm{ND}) = (P - P_o)/P_m, Y(\mathrm{NA}) = (P_m - P'_m)/P_m$$

Isolation of intact chloroplasts, soluble proteins, and total thylakoid membranes

Intact chloroplasts, soluble proteins, and total thylakoid membranes were isolated from 3-week-old plants using the method described in our previous study (Zhong *et al.*, 2013).

Isolation of intact thylakoid membranes, grana-enriched and stroma lamellae-enriched thylakoid membranes

Intact thylakoid membranes were isolated using the method described in Peng and Shikanai (2011). Grana-enriched and stroma lamellae-enriched thylakoid membranes were prepared according to the method described by Lu *et al.* (2011).

Protease protection assays and chaotropic agent washing of intact thylakoid membranes

The assay to determine the extent of protection of the intact thylakoid membrane from protease was conducted as previously reported (Meurer *et al.*, 1998). For experiments involving washing with a chaotropic agent, intact thylakoid membranes with a final concentration of 50 mg chlorophyll/mL were incubated with various chaotropic agents (1 M NaCl, 1 M $CaCl_2$, 0.2 M Na_2CO_3, and 6 M urea) for 30 min. Then, the thylakoid membranes were pelleted at 100 000 ***g*** for 2 h at 4°C, washed with isolation buffer, and used for immunoblot analysis.

Immunoblot, SDS-PAGE, and BN-PAGE analyses

For immunoblot analysis, total leaf proteins or thylakoid membrane proteins were separated using 15% SDS-PAGE containing 6 M urea. After electrophoresis, proteins were transferred onto polyvinylidene fluoride (PVDF) membranes (GE Healthcare, USA). The membranes were then probed with specific antibodies and visualized using the enhanced chemiluminescence method. Antibodies for PsaC (AS10939, LOT 1502), PsaE (AS08324A, LOT 1602), Lhca1 (AS01005, LOT 1310), and Lhca2 (AS01006, LOT 1403) were purchased from Agrisera (Sweden).The Pyg7 antibody was raised against the N-NKVARPRRDALKDRVK-C peptide. All other antibodies were produced in our laboratory (Liu *et al.*, 2012). BN-PAGE was performed according to the method described in Peng *et al.* (2008).

Suc gradient fractionation of thylakoid membranes

Leaves from WT and *ppd1* plants were homogenized with extraction buffer (10 mM HEPES-KOH, pH 7.6, 5 mM $MgCl_2.6H_2O$, 0.4 M sucrose, 10 mM NaCl). The homogenate was filtered through miracloth (Calbiochem, Germany) before being centrifuged at 5000 rpm for 10 min at 4°C. Pellets were washed and solubilized

with 1% (w/v) n-dodecyl-β-DM for 10 min on ice, then centrifuged at 20 000 ***g*** at 4°C for 5 min. The supernatant was loaded on top of a 0.1–1 M continuous sucrose gradient in 5 mM $MgCl_2$, 10 mM NaCl, 0.06% (w/v) DM, and 25 mM MES-NaOH, pH 5.7. After centrifugation for 22 h at 160 000 ***g*** at 4°C using an SW40 Ti rotor (Beckman, USA), 20 fractions were collected from the bottom of the gradient and characterized by immunoblot analysis.

In vivo pulse and chase labeling of chloroplast proteins

Proteins were labeled *in vivo* as described by Meurer *et al.* (1998). The first true leaves from 10-day-old seedlings were pre-incubated in the presence of 20 mg ml^{-1} cycloheximide for 30 min, then labeled with 1 μCi μl^{-1} [^{35}S]Met (specific activity >1000 Ci $mmol^{-1}$, Amersham Pharmacia Biotech) for different periods of time at 25°C. The pulse-labeled leaves were chased in the presence of 10 mM unlabeled methionine for different periods of time. Thylakoid membranes isolated from labeled leaves were subjected to BN-PAGE analysis.

Isolation of the PSI core complex

The PSI core complex was isolated according to the method described by Qin *et al.* (2015b).

Subcellular localization of GFP fusion proteins

Full-length *Pyg7* cDNA was cloned into the pBI221-P35S-GFP vector to express the Pyg7-GFP fusion protein (for primers used, see Table S1). Constructs for nuclear, chloroplast, and mitochondrion localization were described previously (Liu *et al.*, 2012; Zhong *et al.*, 2013). Constructs and the empty vector were transformed into *Arabidopsis* protoplasts. GFP images were examined using a confocal laser scanning microscope (TCS SP5, Leica, Germany).

Bimolecular fluorescence complementation (BiFC)

BiFC assays were performed according to the method described by Walter *et al.* (2004). Full-length *Pyg7* cDNA was ligated into pUC-SPYNE. The full-length cDNAs of *PsaD* and *PsaE* were subcloned into pUC-SPYCE. The full-length *PsaC* cDNA was introduced into pUC-SPYCE vector connected with the *RbcS 1A* signal peptide (amino acids 1–54). Constructs were co-transformed into protoplasts (for primers used for fusion constructs, see Table S1). YFP fluorescence was imaged using a confocal laser scanning microscope (TCS SP5, Leica, Germany).

Yeast two-hybrid and protein overlay assays

Yeast two-hybrid analyses were performed using the GAL4 two-hybrid system (TaKaRa, Japan), as described in our previous study (Liu *et al.*, 2012). Sequences encoding the N-terminal region of *Pyg7* (amino acids 62–85) and the C-terminal region containing TPR domains (amino acids 142–301) were amplified. The resulting DNA fragments were cloned into pGBKT7 (DNA-binding domain) and used as bait. The PsaC coding sequence was subcloned into pGADT7 (activation domain) and used as prey. Primers used are listed in Table S1. Direct interaction between two proteins was investigated by cotransforming the respective plasmid constructs into yeast reporter strain Y187. A protein overlay assay was carried out according to previously described methods (Naver *et al.*, 2001; Liu *et al.*, 2012). A chromogenic western blot immunodetection kit (Catalog number WB7103, Thermo fisher, USA) was used for detection of Pyg7-His. The same nitrocellulose membrane was probed with PsaC antibody and visualized by the enhanced chemiluminescence method.

PSI stability analysis

Leaves detached from 4-week-old WT and *i1* seedlings were pre-incubated with lincomycin (100 mg ml^{-1}) and cycloheximide (20 mg ml^{-1}) to inhibit chloroplast-encoded and nuclear-encoded protein synthesis, respectively, for 30 min in the dark. Next, the leaves were exposed to 80 μmol m^{-2} sec^{-1} (moderate light, i.e. growth light) and 250 μmol m^{-2} sec^{-1} (excess light) for various periods of time up to 30 h at 25°C. Maximum photo-oxidizable P700, maximum photochemical efficiency of PSII (F_v/F_m), and levels of PSI subunits (PsaA, PsaC, and PsaD), the PSII subunit D2, and the cytochrome b6f complex subunit PetD were followed during light treatments.

Complementation of the *pyg7* mutant

The full-length *Pyg7* coding sequence was cloned into the pCAMBIA1301 vector and mobilized into *Agrobacterium tumefaciens* strain GV3101. Heterozygous *pyg7* was transformed using the floral-dip method (Clough and Bent, 1998). Transgenic plants were selected on MS medium containing 50 mg L^{-1} hygromycin.

ACCESSION NUMBERS

Sequence data from this article can be found in the Arabidopsis Genome Initiative data library under the following accession numbers: *Pyg7* (AT1G22700), *PsaA* (ATCG00350), *PsaB* (ATCG00340), *PsaC* (ATCG01060), *PsaD* (AT4G02770), *PsaE* (AT4G28750), *PsaF* (AT1G31330), *PsaG* (AT1G55670), *Lhca1* (AT3G54890), *Lhca2* (AT3G61470), *Lhcb1* (AT1G29920), *D1* (ATCG00020), *D2* (ATCG00270), *CP43* (ATCG00280), *CP47* (ATCG00680), *PsbO* (AT5G66570), *PetA* (ATCG00540), *PetD* (ATCG00730), *CF1*β (ATCG00480), *RbcS 1A* (AT1G67090), *Ycf3* (ATCG00360), *Ycf4* (ATCG00520), *Y3IP1* (AT5G44650), and *Actin* (AT3G18780).

ACKNOWLEDGEMENTS

We are grateful to the ABRC for seed stocks. This work was supported by the National Natural Science Foundation of China (reference number 31300994), the Key Research Plan of Frontier Sciences of the Chinese Academy of Sciences (reference number QYZDJ-SSW-SMC003) and the Strategic Priority Research Program of the Chinese Academy of Sciences (reference number XDB17030300), the State Key Basic Research and Development Plan of China (reference number 2015CB150105), and the National Key Scientific Instrument and Equipment Development Project of China (reference number 2013YQ030595). We would like to thank Dr Xiaochun Qin and Ms Qiujing Yan for their help during isolation of the PSI core complex.

CONFLICT OF INTEREST

The authors declare no conflicts of interest.

AUTHOR CONTRIBUTIONS

H.Y., P.L., and C.L. designed the study; H.Y., P.L., and A.Z. performed the research; X.W., L.Z., and C.L. analysed the data; H.Y., P.L., and C.L. wrote the paper.

SUPPORTING INFORMATION

Additional Supporting Information may be found in the online version of this article.

Figure S1. Growth, identification and complementation of the *pyg7* mutant.

Figure S2. Spectroscopic characterization of wild-type, *pyg7*, and *pyg7* com.

Figure S3. Analyses of chloroplast proteins from wild-type, *pyg7*, and *pyg7* com.

Figure S4. Two-dimensional (2D) blue native (BN)/SDS-PAGE analysis of [^{35}S]Met-labeled thylakoid membrane protein complexes.

Figure S5. Two-dimensional (2D) blue native (BN)/SDS-PAGE analysis of the PSI core complex.

Figure S6. Levels of PsaA and Pyg7 during leaf ontogenesis of wild-type plants.

Figure S7. Localization of Pyg7 within chloroplasts using green fluorescent protein (GFP).

Figure S8. Amino acid alignment of *Arabidopsis* Pyg7 and its homologs: Ycf37 from *Synechocystis* sp. PCC6803 and CGL71 from *Chlamydomonas reinhardtii*.

Figure S9. Function and abundance of PSI in *Pyg7* RNAi lines.

Figure S10. PSII stability analysis in the wild-type and *Pyg7* RNAi *i1* line.

Figure S11. Assembly of thylakoid protein complexes in the wild-type and *Pyg7* RNAi line *i1*.

Table S1. List of primers used in this study.

REFERENCES

Albus, C.A., Ruf, S., Schöttler, M.A., Lein, W., Kehr, J. and Bock, R. (2010) Y3IP1, a nucleus-encoded thylakoid protein, cooperates with the plastid-encoded Ycf3 protein in photosystem I assembly of tobacco and *Arabidopsis*. *Plant Cell*, **22**, 2838–2855.

Amunts, A. and Nelson, N. (2008) Functional organization of a plant photosystem I: evolution of a highly efficient photochemical machine. *Plant Physiol. Biochem.* **46**, 228–237.

Amunts, A. and Nelson, N. (2009) Plant photosystem I design in the light of evolution. *Structure*, **17**, 637–650.

Armbruster, U., Zühlke, J., Rengstl, B. *et al.* (2010) The Arabidopsis thylakoid protein PAM68 is required for efficient D1 biogenesis and photosystem II assembly. *Plant Cell*, **22**, 3439–3460.

Blatch, G.L. and Lässle, M. (1999) Thetetratricopeptide repeat: a structural motif mediating protein–protein interactions. *BioEssays*, **21**, 932–939.

Bohne, A.-V., Schwenkert, S., Grimm, B. and Nickelsen, J. (2016) Roles of tetratricopeptide repeat proteins in biogenesis of the photosynthetic apparatus. *Int. Rev. Cell Mol. Biol.* **324**, 187–227.

Boudreau, E., Takahashi, Y., Lemieux, C., Turmel, M. and Rochaix, J.-D. (1997) The chloroplast ycf3 and ycf4 open reading frames of *Chlamydomonas reinhardtii* are required for the accumulation of the photosystem I complex. *EMBO J.* **16**, 6095–6104.

Busch, A. and Hippler, M. (2011) The structure and function of eukaryotic photosystem I. *Biochim. Biophys. Acta (BBA)-Bionerg.* **1807**, 864–877.

Clough, S.J. and Bent, A.F. (1998) Floral dip: a simplified method for *Agrobacterium*-mediated transformation of *Arabidopsis thaliana*. *Plant J.* **16**, 735–743.

Das, A.K., Cohen, P.W. and Barford, D. (1998) The structure of the tetratricopeptide repeats of protein phosphatase 5: implications for TPR-mediated protein–protein interactions. *EMBO J.* **17**, 1192–1199.

Dühring, U., Irrgang, K.D., Lünser, K., Kehr, J. and Wilde, A. (2006) Analysis of photosynthetic complexes from a cyanobacterial *ycf37* mutant. *Biochim. Biophys. Acta (BBA)-Bionerg.* **1757**, 3–11.

Dühring, U., Ossenbühl, F. and Wilde, A. (2007) Late assembly steps and dynamics of the cyanobacterial photosystem I. *J. Biol. Chem.* **282**, 10915–10921.

Gleave, A.P. (1992) A versatile binary vector system with a T-DNA organisational structure conducive to efficient integration of cloned DNA into the plant genome. *Plant Mol. Biol.* **20**, 1203–1207.

Göhre, V., Ossenbühl, F., Crèvecoeur, M., Eichacker, L.A. and Rochaix, J.D. (2006) One of two Alb3 proteins is essential for the assembly of the photosystems and for cell survival in *Chlamydomonas*. *Plant Cell*, **18**, 1454–1466.

Heinnickel, M., Kim, R.G., Wittkopp, T.M., Yang, W., Walters, K.A., Herbert, S.K. and Grossman, A.R. (2016) Tetratricopeptide repeat protein protects photosystem I from oxidative disruption during assembly. *Proc. Natl Acad. Sci. USA*, **113**, 2774–2779.

Jagannathan, B. and Golbeck, J.H. (2009) Understanding of the binding interface between PsaC and the PsaA/PsaB heterodimer in photosystem I. *Biochemistry*, **48**, 5405–5416.

Kargul, J., Janna Olmos, J.D. and Krupnik, T. (2012) Structure and function of photosystem I and its application in biomimetic solar-to-fuel systems. *J. Plant Physiol.* **169**, 1639–1653.

Klughammer, C. and Schreiber, U. (2008) Saturation pulse method for assessment of energy conversion in PSI. *PAM Application Notes*, **1**, 11–14.

Krech, K., Ruf, S., Masduki, F.F., Thiele, W., Bednarczyk, D., Albus, C.A., Tiller, N., Hasse, C., Schöttler, M.A. and Bock, R. (2012) The plastid genome-encoded Ycf4 protein functions as a non-essential assembly factor for photosystem I in higher plants. *Plant Physiol.* **159**, 579–591.

Liu, J., Yang, H., Lu, Q., Wen, X., Chen, F., Peng, L., Zhang, L. and Lu, C. (2012) PsbP-domain protein1, a nuclear-encoded thylakoid lumenal protein, is essential for photosystem I assembly in *Arabidopsis*. *Plant Cell*, **24**, 4992–5006.

Lu, Y., Hall, D.A. and Last, R.L. (2011) A small zinc finger thylakoid protein plays a role in maintenance of photosystem II in *Arabidopsis thaliana*. *Plant Cell*, **23**, 1861–1875.

Mazor, Y., Borovikova, A. and Nelson, N. (2015) The structure of plant photosystem I super-complex at 2.8 Å resolution. *Elife*, **4**, e07433.

Meurer, J., Meierhoff, K. and Westhoff, P. (1996) Isolation of high-chlorophyll-fluorescence mutants of *Arabidopsis thaliana* and their characterisation by spectroscopy, immunoblotting and northern hybridisation. *Planta*, **198**, 385–396.

Meurer, J., Plücken, H., Kowallik, K.V. and Westhoff, P. (1998) A nuclear-encoded protein of prokaryotic origin is essential for the stability of photosystem II in *Arabidopsis thaliana*. *EMBO J.* **17**, 5286–5297.

Naver, H., Boudreau, E. and Rochaix, J.-D. (2001) Functional studies of Ycf3: its role in assembly of photosystem I and interactions with some of its subunits. *Plant Cell*, **13**, 2731–2745.

Nelson, N. (2009) Plant photosystem I-the most efficient nano-photochemical machine. *J. Nanosci. Nanotechnol.* **9**, 1709–1713.

Onishi, T. and Takahashi, Y. (2009) Effects of site-directed mutations in the chloroplast-encoded *ycf4* gene on PSI complex assembly in the green alga *Chlamydomonas reinhardtii*. *Plant Cell Physiol.* **50**, 1750–1760.

Ozawa, S., Onishi, T. and Takahashi, Y. (2010) Identification and characterization of an assembly-intermediate subcomplex of photosystem I in the green alga *Chlamydomonas reinhardtii*. *J. Biol. Chem.* **285**, 20072–20079.

Peng, L. and Shikanai, T. (2011) Supercomplex formation with photosystem I is required for the stabilization of the chloroplast NADH dehydrogenase-like complex in Arabidopsis. *Plant Physiol.* **155**, 1629–1639.

Peng, L., Shimizu, H. and Shikanai, T. (2008) The chloroplast NAD(P)H dehydrogenase complex interacts with photosystem I in *Arabidopsis*. *J. Biol. Chem.* **283**, 34873–34879.

Pfündel, E., Klughammer, C. and Schreiber, U. (2008) Monitoring the effects of reduced PSII antenna size on quantum yields of photosystems I and II using the Dual-PAM-100 measuring system. *PAM Application Notes*, **1**, 21–24.

Qin, X., Suga, M., Kuang, T. and Shen, J.R. (2015a) Structural basis for energy transfer pathways in the plant PSI-LHCI supercomplex. *Science*, **348**, 989–995.

Qin, X., Wang, W., Chang, L., Chen, J., Wang, P., Zhang, J., He, Y., Kuang, T. and Shen, J.R. (2015b) Isolation and characterization of a PSI-LHCI super-complex and its sub-complexes from a siphonaceous marine green alga, *Bryopsis Corticulans*. *Photosynth. Res.* **123**, 61–76.

Roose, J.L., Frankel, L.K. and Bricker, T.M. (2014) The PsbP domain protein 1 functions in the assembly of lumenal domains in photosystem I. *J. Biol. Chem.* **289**, 23776–23785.

Ruf, S., Kössel, H. and Bock, R. (1997) Targeted inactivation of a tobacco intron-containing open reading frame reveals a novel chloroplast-encoded photosystem I-related gene. *J. Cell Biol.* **139**, 95–102.

Scheufler, C., Brinker, A., Bourenkov, G., Pegoraro, S., Moroder, L., Bartunik, H., Hartl, F.U. and Moarefi, I. (2000) Structure of TPR domain-peptide complexes: critical elements in the assembly of the Hsp70-Hsp90 multichaperone machine. *Cell*, **101**, 199–210.

Schöttler, M.A. and Tóth, S.Z. (2014) Photosynthetic complex stoichiometry dynamics in higher plants: environmental acclimation and photosynthetic flux control. *Front. Plant Sci.* **5**, 188.

Schöttler, M.A., Albus, C.A. and Bock, R. (2011) Photosystem I: its biogenesis and function in higher plants. *J. Plant Physiol.* **168**, 1452–1461.

Schwabe, T.M., Gloddek, K., Schluesener, D. and Kruip, J. (2003) Purification of recombinant BtpA and Ycf3, proteins involved in membrane protein biogenesis in *Synechocystis* PCC 6803. *J. Chromatogr. B*, **786**, 45–59.

Shen, J., Williams-Carrier, R. and Barkan, A. (2017) PSA3, a protein on the stromal face of the thylakoid membrane, promotes photosystem I accumulation in cooperation with the assembly factor PYG7. *Plant Physiol.* **174**, 1850–1862.

Shikanai, T. (2007) Cyclic electron transport around photosystem I: genetic approaches. *Annu. Rev. Plant Biol.* **58**, 199–217.

Stöckel, J., Bennewitz, S. and Oelmüller, R. (2006) The evolutionarily conserved tetratrico peptide repeat protein Pale Yellow Green7 is required for photosystem I accumulation in *Arabidopsis* and copurifies with the complex. *Plant Physiol.* **141**, 870–878.

Suga, M., Qin, X., Kuang, T. and Shen, J.R. (2016) Structure and energy transfer pathways of the plant photosystem I-LHCI supercomplex. *Curr. Opin. Struct. Biol.* **39**, 46–53.

Suorsa, M., Rantala, M., Mamedov, F., Lespinasse, M., Trotta, A., Grieco, M., Vuorio, E., Tikkanen, M., Järvi, S. and Aro, E.M. (2015) Light acclimation involves dynamic re-organization of the pigment-protein megacomplexes in non-appressed thylakoid domains. *Plant J.* **84**, 360–373.

Suzuki, K., Ohmori, Y. and Ratel, E. (2011) High root temperature blocks both linear and cyclic electron transport in the dark during chilling of the leaves of rice seedlings. *Plant Cell Physiol.* **52**, 1697–1707.

Takahashi, Y., Goldschmidt-Clermont, M., Soen, S.Y., Franzén, L.G. and Rochaix, J.-D. (1991) Directed chloroplast transformation in *Chlamydomonas reinhardtii*: insertional inactivation of the psaC gene encoding the iron sulfur protein destabilizes photosystem I. *EMBO J.* **10**, 2033–2040.

Tiwari, A., Mamedov, F., Grieco, M., Suorsa, M., Jajoo, A., Styring, S., Tikkanen, M. and Aro, E.M. (2016) Photodamage of iron-sulphur clusters in photosystem I induces non-photochemical energy dissipation. *Nat. Plants*, **2**, 16035.

Walter, M., Chaban, C., Schütze, K. *et al.* (2004) Visualization of protein interactions in living plant cells using bimolecular fluorescence complementation. *Plant J.* **40**, 428–438.

Wang, L., Li, Q., Zhang, A. *et al.* (2017) The phytol phosphorylation pathway is essential for the biosynthesis of phylloquinone, which is required for photosystem I stability in *Arabidopsis*. *Mol. Plant*, **10**, 183–196.

Watkins, K.P., Rojas, M., Friso, G., van Wijk, K.J., Meurer, J. and Barkan, A. (2011) APO1 promotes the splicing of chloroplast group II introns and harbors a plant-specific zinc-dependent RNA binding domain. *Plant Cell*, **23**, 1082–1092.

Wesley, S.V., Helliwell, C.A., Smith, N.A. *et al.* (2001) Construct design for efficient, effective and high-throughput gene silencing in plants. *Plant J.* **27**, 581–590.

Wilde, A., Lünser, K., Ossenbühl, F., Nickelsen, J. and Börner, T. (2001) Characterization of the cyanobacterial *ycf37*: mutation decreases the photosystem I content. *Biochemistry*, **357**, 211–216.

Wollman, F.A., Minai, L. and Nechushtai, R. (1999) The biogenesis and assembly of photosynthetic proteins in thylakoid membranes. *Biochim. Biophys. Acta (BBA)-Bionerg.* **1411**, 21–85.

Wostrikoff, K., Girard-Bascou, J., Wollman, F.A. and Choquet, Y. (2004) Biogenesis of PSI involves a cascade of translational autoregulation in the chloroplast of *Chlamydomonas*. *EMBO J.* **23**, 2696–2705.

Yang, H., Liu, J., Wen, X. and Lu, C. (2015) Molecular mechanism of photosystem I assembly in oxygenic organisms. *Biochim. Biophys. Acta (BBA)-Bionerg.* **1847**, 838–848.

Yu, J., Smart, L.B., Jung, Y.S., Golbeck, J. and McIntosh, L. (1995) Absence of PsaC subunit allows assembly of photosystem I core but prevents the binding of PsaD and PsaE in *Synechocystis* sp. PCC6803. *Plant Mol. Biol.* **29**, 331–342.

Zhong, L., Zhou, W., Wang, H., Ding, S., Lu, Q., Wen, X., Peng, L., Zhang, L. and Lu, C. (2013) Chloroplast small heat shock protein HSP21 interacts with plastid nucleoid protein pTAC5 and is essential for chloroplast development in *Arabidopsis* under heat stress. *Plant Cell*, **25**, 2925–2943.

